Ground state of the fermion one-component plasma: A Monte Carlo study in two and three dimensions

D. Ceperley*
Laboratoire de Physique Theorique et Hautes Energies, Université de Paris XI, Orsay, France
(Received 26 April 1978)

We have performed fermion Monte Carlo variational calculations to determine the equation of state of the uniform electron one-component plasma in two and three dimensions. The ground-state excess energies calculated by the Monte Carlo method are very precise and in agreement with those of other calculations in the metallic density range and in the very-low-density Wigner crystals. Three phases have been investigated: the Wigner crystal, the normal or unpolarized fluid, and the polarized fluid. The Wigner crystal has the lowest energy for $r_s > 67$ in three dimensions and $r_s > 33$ in two dimensions. The totally polarized quantum fluid is stable for $26 < r_s < 67$ in three dimensions and for $13 < r_s < 33$ in two dimensions, and the normal or unpolarized fluid is stable at higher densities, $r_s < 26$ in three dimensions and $r_s < 13$ in two dimensions. A pseudopotential with no adjustable parameters, derived from the random-phase approximation, is found to give excellent energies. The present results lend support to earlier conjectures that the ground state of the electron gas will be spin polarized at intermediate densities.

I. INTRODUCTION

In this paper we will give results which depend on the computational techniques now available to obtain a variational bound for the ground-state energy of the fermion plasma. The quantum plasma with a uniform neutralizing background is a widely used model in many-body physics. The most common application is to free electrons in metals and semiconductors. But if hydrogen is compressed to very high densities, as in a white dwarf, the electrons become a relativistic uniform background while the protons constitute a cold plasma.[1]

In recent years several two-dimensional (2D) plasma systems have become of interest. Electrons trapped above the surface of liquid helium[2] are nearly a perfect realization of the 2D one-component plasma since the movement in the direction perpendicular to the surface is very much smaller than the electron spacing. The surface charge density can be varied over many orders of magnitude by changing the electric field perpendicular to the surface. Another example of a system that can be fruitfully modeled by a 2D quantum plasma is the inversion layer[3] between a semiconductor and metal oxide.

The phases of the one-component plasma have received a great deal of attention since Wigner[4] pointed out that the plasma would crystallize at sufficiently low density and temperature in order to minimize the potential energy. The transition density at $T = 0$ is still unknown. Estimates of the density vary over six orders of magnitude.[5] Determination of the transition density is difficult because the energies of both the crystal and the strongly coupled fluid must be determined to high accuracy (1 part in 10^4).

At high density the plasma will become an ideal Fermi gas in order to minimize the kinetic energy. It has been suggested, originally by Bloch,[6] that at intermediate densities a locally polarized state with all the spins aligned, will have a lower energy than the normal fluid. Again estimates of this phase transition are rather scattered.[7,8] Other states such as spin-density waves,[8,9] have been proposed for the ground state. In this paper we will consider only three phases: the crystal, the normal or unpolarized fluid, and the completely polarized fluid.

The Monte Carlo variational method has been successfully applied to both isotopes of helium[10] and neutron matter.[11] One assumes that the wave function is well approximated by the product trial function and then one minimizes the variational energy with respect to the correlation function.[12] The integrals which arise in finding the variational energy are calculated by the Metropolis[13] random-walk algorithm.

II. PRELIMINARIES

In this paper lengths will be given in units of a, where a is the radius of a sphere (circle in two dimensions) which encloses on the average one particle.

$$a = \begin{cases} (\pi\rho)^{-1/2}, & d = 2 \\ (4\pi\rho/3)^{-1/3}, & d = 3 \end{cases} \tag{1}$$

and ρ is the number density. Energies will be given in Rydbergs ($\hbar^2/2ma_0^2$), where a_0 is the Bohr radius: $a_0 = \hbar^2/me^2$. In these units the Hamilton-

ian is

$$H=\frac{1}{r_s^2}\sum_{i=1}^{N}\nabla_i^2+\frac{2}{r_s}\sum_{i<j}^{N}\frac{1}{|\vec{r}_i-\vec{r}_j|}\,, \tag{2}$$

where $r_s=a/a_0$ and N is the number of particles in the simulation, d is the dimensionality (either two or three). The Fourier transform of a function $u(r)$ is normalized as

$$u(\vec{k})=\rho\int_0^L dr^d\, e^{i\vec{k}\cdot\vec{r}}u(\vec{r})\,, \tag{3}$$

where L is the side of the simulation cube (square in two dimensions). R will symbolize the set of $3N$ particle coordinates.

III. VARIATIONAL TRIAL FUNCTION

In this paper we will assume the trail function is of the Bijl-Dingle-Jastrow[14] or product form:

$$\Psi_T(R)=D(R)\exp\left(-\sum_{i<j}^{N}u(|\vec{r}_i-\vec{r}_j|)\right). \tag{4}$$

The function $D(R)$ is the "model" noninteracting term and serves to give the trail function the desired antisymmetry. For the fluid phase we take $D(R)$ to be a Slater determinant of plane waves. In the unpolarized fluid there are separate determinants for spin-up and spin-down particles. For the polarized fluid there is a single determinant. In the crystal phase $D(R)$ is a Slater determinant of single-particle orbitals centered around the lattice sites. The "pseudopotential," $u(r)$ is repulsive and includes in an approximate way the effects of particle correlation.

IV. PSEUDOPOTENTIAL

The ground-state energy of a quantum system is known from other studies[12,15] to be not very sensitive to the choice of the pseudopotential $u(r)$. However, if the form of $u(r)$ is chosen carefully an expensive and tedious search for the optimal pseudopotential [which we will denote $u^*(r)$] can be avoided. Let us review what is known about the long- and short-range behavior of $u^*(r)$.

For small r, u^* will be finite but large: The value of the derivative of u^* is given by the cusp condition[16]:

$$\lim_{r\to 0}\frac{du^*(r)}{dr}=-[r_s(d\pm 1)]^{-1}\,, \tag{5}$$

where the upper sign is to be used if the particles have the same spin, the lower sign for opposite spins. There is less correlation needed between parallel spins since the Slater determinant already provides some repulsion. In this paper we shall limit ourselves to pseudopotentials which are independent of relative spin. With this constraint, the upper sign in Eq. (5) should be used for the unpolarized liquid, the lower sign for the polarized liquid.

The zero-point motion of the plasmons determines the behavior of u^* at large r. Various approaches[17,18] show that the pseudopotential will be long ranged in order to screen out the Coulomb interaction. In fact

$$\lim_{r\to\infty}u^*(r)=\begin{cases}1.4793(r_s/r)^{1/2}\,, & d=2\\ (\frac{1}{3}r_s)^{1/2}/r\,, & d=3\,.\end{cases} \tag{6}$$

We shall derive these limiting forms in discussing the crystal pseudopotential.

Gaskell[19] has found a pseudopotential which combines both the small- and large-r behavior. First he assumes that the structure function for the interacting liquid $S(k)$ is close to that of the noninteracting liquid and for a small pseudopotential, $u(r)$, can be approximated by the perturbation formula

$$S(k)=[1/S_0(k)+2u(k)]^{-1}\,, \tag{7}$$

where $u(k)$ is the Fourier transform of $u(r)$. The variational energy in the random-phase approximation (RPA) (i.e., neglecting three phonon terms) can then be minimized with respect to $u(k)$ to yield

$$2u_{\mathrm{RPA}}(k)=-\frac{1}{S_0(k)}+\left(\frac{1}{S_0(k)^2}+\frac{4V(k)m}{\hbar^2k^2}\right)^{1/2}, \tag{8}$$

where $V(k)$ is the Fourier transform of the interparticle potential. Tallman[20] introduces a variational expansion procedure and gets the same form to lowest order. Krotscheck[21] has shown that the lowest-order terms in the small-k expansion are correctly given by Eq. (8).

As a comparison we have performed calculations with a pseudopotential which is a difference of Yukawa's.

$$u_Y(r)=Ae^{-Br}(1-e^{-r/F})/r\,. \tag{9}$$

This function has been used with good results to study neutron matter[22] and with $B=0$ the electron gas.[23-25]

V. CRYSTAL TRIAL FUNCTION

In quantum variational calculations for the crystal phase it has been found necessary[26] to explicitly bind the particles to the crystal lattice sites with single-particle orbitals $\phi(r)$. We follow the usual practice and take $\phi(r)$ to be a Gaussian,

$$\phi(r)=e^{-Cr^2}\,, \tag{10}$$

although this function does not have the correct behavior[27] for large r.

Lattice dynamics shows that the stable crystal

type in three dimensions[28] is body centered cubic (bcc) and in two dimensions[29] is the triangular lattice. We have used these lattice types exclusively in our simulations. Let $\{\vec{R}_i\}$ be the set of lattice points. The crystal trial function is

$$\Psi_T(R) = \exp\left(-\sum_{i<j} u(r_{ij})\right) \sum_{P\in S(P)} (-1)^P \prod_{i=1}^{N} \phi(\vec{r}_i - \vec{R}_{P_i}) , \tag{11}$$

where $S(P)$ is the set of permutations allowed. In our simulations we have used three choices for $S(P)$: (a) the Boltzmann crystal is achieved by allowing only the unit permutation; i.e., one does not antisymmetrize. (b) In the antiferromagnetic or unpolarized crystal the lattice is divided into a spin-up lattice, occupying the corners of the bcc lattice, and a spin-down lattice, occupying the body sites. $S(P)$ consists of the set of permutations which preserve the spin of a site. (c) In the ferromagnetic or polarized crystal $S(P)$ consists of all permutations.

Because the particles are localized about the lattice sites, we need a pseudopotential which is less repulsive than u_{RPA}. The optimal pseudopotential in the low-density limit can be calculated as follows: if the particles are well localized the permutations in Eq. (11) are unimportant and we can use the Boltzmann form (a) with the Gaussian orbital. The local trial energy defined as

$$E_T(R) = \Psi_T^{-1}(R) H(R) \Psi_T(R) \tag{12}$$

can be written in terms of collective coordinates and displacements from crystal sites as

$$\begin{aligned} E_T(R) = &\frac{1}{2N}\sum_k (\rho_k^2 - N)\left(v_k - u_k k^2 \frac{\hbar^2}{m}\right) + \frac{dC\hbar^2}{m} \\ &- \frac{\hbar^2}{2m}\left(4C^2 \sum_i (\vec{r}_i - \vec{R}_i)^2 \right. \\ &+ \frac{4Ci}{N}\sum_{ki} u_k \rho_k^* e^{i\vec{k}\cdot\vec{r}}\, \vec{k}\cdot(\vec{r}_i - \vec{R}_i) \\ &\left. + \frac{1}{N^2}\sum_{kk'} u_k u_{k'} \vec{k}\cdot\vec{k}'\, \rho_k^* \rho_{k'} \rho_{k-k'}\right), \end{aligned} \tag{13}$$

where u_k and v_k are the Fourier transforms of the pseudopotential and potential, respectively, (8) and ρ_k are the collective coordinates

$$\rho_k = \sum_{i=1}^{N} e^{i\vec{k}\cdot\vec{r}_i} . \tag{14}$$

Now if $\Psi_T(R)$ were a solution of Schrödinger's equation $E_T(R)$ would be constant independent of the collective coordinates and particle displacements. In the spirit of the random-phase approximation we make $E_T(R)$ invariant under the presence of exactly one phonon; this will determine a unique $u(r)$.

Let the particle displacement be given by

$$\vec{r}_i - \vec{R}_i = -\epsilon\vec{q}\sin(\vec{q}\cdot\vec{R}_i)/q^2 . \tag{15}$$

Then for k and q less than a reciprocal-lattice vector and ϵ small it is easy to show that

$$\rho_k = -i\epsilon/2(\delta_{k-q} + \delta_{k+q}) + O(\epsilon^2) , \tag{16}$$

and the local energy as defined in Eq. (12) is

$$\begin{aligned} E_T(R) = &E_T(R, \epsilon = 0) \\ &+ \tfrac{1}{4}\epsilon^2 N\left[v_q - \frac{\hbar^2}{m}\left((q^2 u_q + q^2 u_q^2 + 4\frac{C^2}{q^2} + 4Cu_q\right)\right] \\ &+ O(\epsilon^4) . \end{aligned} \tag{17}$$

Then the pseudopotential $u_c(r)$ which will make this energy independent of ϵ and $\vec{q}$ is

$$2u_c(\vec{q}) = -1 - 4C/q^2 + (1 + 8C/q^2 + 4m v_q/\hbar^2 q^2)^{1/2} . \tag{18}$$

Note that this function equals u_{RPA} for a Bose liquid ($S_0 = 1$) when $C = 1$. We have succeeded in constructing a pseudopotential which is less repulsive than u_{RPA}. For example, at large r it behaves like

$$u_c(r) = \frac{(\frac{1}{3}r_s)^{1/2} - \frac{1}{3}2C}{r} , \quad r \gg 1 , \quad d = 3 . \tag{19}$$

Our simulations show that the optimal value of C is given approximately by $C^* = 0.2 r_s^{1/2}$. Then in three dimensions the binding to the lattice site reduces the long-range part of the pseudopotential by about 25%.

The situation in two dimensions is quite different. The second term in $u_c(q)$, $-4C/q^2$, diverges too quickly at $q = 0$ for the Fourier transform to exist. This is because a two-dimensional crystal is unstable under the influence of phonons in the thermodynamic limit.[30] Nonetheless the optimal pseudopotential always exists for a finite system; we only need to introduce a cutoff. The pseudopotential we used in two dimensions had the form

$$\begin{aligned} 2u_c(q) = &-1 - 4C/[q^2 + (2\pi/L)^2] \\ &+ (1 + 8C/q^2 + 4m v_q/\hbar^2 q^2)^{1/2} . \end{aligned} \tag{20}$$

With this cutoff $u_c(r)$ contains a term, $-C\ln(r\pi/L)$, for $r \ll L$ which diverges very slowly as L becomes large.

The cusp condition is satisfied by u_c in two but not in three dimensions, (where it is in error by 5%). It is rather remarkable that such a simple argument produces so reasonable a pseudopotential. We shall see that the variational energies of u_{RPA} and u_c are nearly optimal.

VI. MONTE CARLO SIMULATION

Monte Carlo simulation has been shown[12] to be a powerful way to calculate the ground-state pro-

perties of many-body quantum systems. Within the variational approximation it is essentially exact since the errors which arise can be accurately assessed. The basic idea is quite simple. In order to calculate any ground-state property using the trial function $\Psi_T(R)$ it is sufficient to be able to sample configurations drawn from the probability density function $|\Psi_T(R)|^2/\int dR|\Psi_T(R)|^2$. The Metropolis[13] algorithm is used to carry out the sampling of this distribution. It consists of a random walk through the $3N$-dimensional configuration space, where each particle is moved one at a time and the moves are either accepted to rejected depending on the relative square of the trial function at the new point. After the walk reaches "equilibrium" typically 50 to 200 moves per particle averages are kept, the most important being the variational energy. It takes another 250 to several thousand steps per particle to get good values for the energy. This method has been extensively used to simulate classical ensembles and was applied by McMillan to compute the ground-state energy of liquid helium. Reference 11 gives technical details on the application of the Monte Carlo method to fermion systems and on how to judge the reliability and accuracy of the calculation.

The electron gas has both a long-range potential $v(r)$ and pseudopotential $u(r)$. We have followed the usual way of treating this problem in computer simulations.[31] Periodic boundary conditions are applied in all dimensions and the system is periodically extended. Then the total potential energy is equal to the sum of the interactions inside the original cell plus the interaction between the original cell and all of the "images" in the extended space minus a background term. The pseudopotential is treated in the same way. The details of how to treat this rather complex interaction numerically are given in the Appendix.

VII. RESULTS OF THE MONTE CARLO CALCULATIONS

We have performed an extensive series of Monte Carlo random walks in both two and three dimensions, with the three different pseudopotentials and with the polarized, unpolarized, and crystal trial functions. The energies from these calculations appear in Table I–III. Later we will correct these energies for their dependence on N, the number of particles in the simulation.

Table I contains the energies of the liquid as calculated with the u_{RPA} pseudopotential, Table II contains the energies with the short-range Yukawa pseudopotential u_Y. In three dimensions the trial parameters A and B are identical to those in Hansen and Mazighi.[32] In two dimensions they have

TABLE I. The Monte Carlo energy per particle as a function of density computed with the pseudopotential from the random-phase approximation [Eq. (8)]. The numbers in parentheses are the standard errors in the last digit. $\bar{k}$ is the rms wave vector; the kinetic energy is given by $(\bar{k}^2/r_s)^2$. The error in $\bar{k}$ is roughly 0.005. $\bar{k}_B$ is $\langle 1/N\sum_{i<j}\nabla^2 u\rangle^{1/2}$, the kinetic energy arising from the correlation portion of the trialfunction. This would equal $\bar{k}$ for a Bose plasma. r_s^* is that value of the density for which $u_{RPA}(r_s^*)$ satisfies the virial relation (see text).

r_s	E/N	$\bar{k}$	$\bar{k}_B$	r_s^*
Two-dimensional unpolarized fluid, $N=58$.				
1.0	−0.429(6)	1.061	0.469	1.2
2.0	−0.515(2)	1.167	0.675	2.3
5.0	−0.2954(6)	1.366	1.010	5.4
10.0	−0.1691(2)	1.572	1.291	10.1
15.0	−0.1188(1)	1.814	1.582	14.6
20.0	−0.09181(6)	1.832	1.601	18.9
30.0	−0.06331(5)	2.005	1.801	27.2
40.0	−0.04847(2)	2.148	1.955	35.4
50.0	−0.03932(4)	2.252	2.078	43.5
100.0	−0.02028(1)	2.667	2.509	83.2
200.0	−0.010390(5)	3.189	3.071	161.
Two-dimensional polarized fluid, $N=57$				
5.0	−0.2842(5)	1.617	1.026	8.9
10.0	−0.1681(1)	1.779	1.302	15.3
15.0	−0.1190(1)	1.893	1.477	19.9
20.0	−0.09209(6)	1.993	1.611	24.7
30.0	−0.06364(4)	2.128	1.797	31.9
50.0	−0.03946(3)	2.362	2.067	49.2
Three-dimensional unpolarized fluid, $N=162$				
1.0	1.108(1)	1.492	0.414	0.8
2.0	−0.0107(5)	1.535	0.598	2.0
3.0	−0.1406(6)	1.584	0.736	3.1
4.0	−0.1584(3)	1.629	0.850	4.3
5.0	−0.1533(3)	1.675	0.950	5.6
7.5	−0.1282(1)	1.788	1.157	8.5
10.0	−0.10672(8)	1.899	1.314	11.5
15.0	−0.07937(9)	2.060	1.552	17.1
20.0	−0.06311(6)	2.201	1.733	22.0
30.0	−0.04493(4)	2.415	1.996	31.3
50.0	−0.02865(1)	2.690	2.347	47.4
75.0	−0.019819(7)	2.946	2.636	64.1
100.0	−0.015208(8)	3.137	2.849	80.0
200.0	−0.007920(3)	3.657	3.411	137.
500.0	−0.003291(1)	4.502	4.308	293.
Three-dimensional polarized fluid, $N=81$				
10.0	−0.1029(2)	2.121	1.284	12.0
30.0	−0.0450(3)	2.522	1.938	37.5
50.0	−0.02885(3)	2.749	2.269	49.7
100.0	−0.015302(7)	3.155	2.768	82.5

TABLE II. Monte Carlo energies and variational parameters computed with the Yukawa pseudopotential u_Y Eq. (9). C is the width of the Gaussians [Eq. (1)] in a crystal trial function. d is the dimensionality, $\bar{k}$ is the rms particle wave vector, γ is Lindemann's ratio (the rms deviation from lattice sites divided by the nearest-neighbor distance).

r_s	N	d	A	B	C	F	E/N	$\bar{k}$	γ
1.0	162	3	0.65	0.0	0.0	0.75	1.115(2)	1.503	
3.0	162	3	1.05	0.0	0.0	0.50	−0.1394(7)	1.633	
10.0	162	3	2.15	0.0	0.0	0.43	−0.10668(7)	1.930	
20.0	162	3	3.2	0.0	0.0	0.41	−0.06317(3)	2.219	
100.0	162	3	8.5	0.0	0.0	0.40	−0.01521(1)	3.353	
1.0	58	2	2.0	0.9	0.0	2.5	−0.422(3)	1.050	
10.0	58	2	4.5	1.15	0.0	0.8	−0.1670(2)	1.578	
20.0	50	2	5.5	0.8	0.0	0.8	−0.0916(1)	1.731	
50.0	50	2	8.0	0.85	0.0	0.4	−0.03920(3)	2.357	
20.0	16	2	5.0	0.8	1.25	0.8	−0.9176(1)	2.128=	0.266
50.0	56	2	6.2	1.1	2.0	0.75	−0.03947(2)	2.515	0.219
100.0	56	2	7.6	0.75	2.7	0.75	−0.02045(1)	2.948	0.185

been found by the reweighting technique.[11] A comparison of the energies in the two tables shows that the differences are very small.[33] Where the difference is greater than one standard error, the energy of u_{RPA} is lower.

Table III contains the crystal energy of the pseudopotential $u_c(r)$. In contrast to the liquid, the solid pseudopotential contains one parameter to be optimized, the localization of the Gaussians C. Finding the optimal value of $C(r_s)$ is quite difficult since the energy has a rather broad and shallow minimum, so that the uncertainty on the optimum value of C is about 20%. Table II contains the results of crystal calculations with u_Y in two dimensions. Again the energies from u_Y are slightly higher than those from u_c.

These results show that the long-range part of the pseudopotential is not very important in determining the ground-state energy. However, our analytic form for the optimal pseudopotential has proved very accurate throughout the density region of interest, and for the remainder of this paper we will use the u_{RPA} pseudopotential in the liquid phase and u_c in the crystal phase. There is a great convenience in performing only a single calculation at each density and N. This gives us energies which are all consistent, and makes fitting the energies to a function throughout the density region easier. Finally, the u_{RPA} pseudopotential has a number of exact limiting behaviors built into it and even though it may not equal the optimal pseudopotential u^*, other properties computed from u_{RPA} such as the structure function or the momentum density may be closer to the ground-state values than those derived from u^*.

We have also performed Monte Carlo calculations with two other potentials in order to test the validity of u_{RPA} more generally. For the Bose one-component plasma the energies of u_{RPA} are the same as those computed by Hansen and Mazighi[32] over a broad energy range. This is to be expected since the pseudopotentials depend little on the statistics of the particles. The other system we investigated was the "Bethe" poten-

TABLE III. Monte Carlo energy for the crystal phase. The pseudopotential is u_C [Eq. (18)], C is the width of the Gaussians [Eq. (10)], pol is the polarization; U unpolarized ($\frac{1}{2}$ spin up, $\frac{1}{2}$ spin down), P is totally polarized, B is the Boltzmann crystal (no antisymmetry). γ is Lindemann's ratio (the ratio of the rms deviation from the nearest lattice site to the nearest-neighbor distance).

r_s	N	Pol	C	E/N	$\bar{k}$	γ
Two-dimensional crystal						
10.0	56	U	0.5	−0.1674(1)	1.767	0.372
15.0	56	U	0.6	−0.1187(1)	1.911	0.346
20.0	56	U	0.7	−0.09198(5)	2.036	0.320
30.0	56	U	0.75	−0.06362(2)	2.206	0.303
40.0	56	U	0.8	−0.04874(2)	2.341	0.297
50.0	56	U	1.0	−0.03955(2)	2.483	0.264
75.0	56	U	1.25	−0.026961(5)	2.733	0.234
100.0	16	U	1.5	−0.02053(2)	2.960	0.216
40.0	56	B	0.8	−0.04874(2)	2.323	0.294
40.0	56	P	0.8	−0.04879(2)	2.361	0.275
Three-dimensional crystal						
30.0	128	U	0.8	−0.044 54(4)	2.513	0.434
50.0	128	U	1.0	−0.028 66(2)	2.842	0.385
50.0	54	B	1.0	−0.028 73(2)	2.802	0.408
50.0	54	U	1.0	−0.028 74(2)	2.822	0.389
50.0	54	P	1.0	−0.028 74(2)	2.892	0.366
100.0	128	U	1.75	−0.015 331(7)	3.469	0.288
200.0	128	U	3.0	−0.008 034(2)	4.255	0.229

tial,[11] a very simplified Yukawa interaction for neutron matter. At high densities, greater than one neutron/F^3, u_{RPA} gives slightly lower energies than u_Y, perhaps because it includes the $1/r^2$ phonon tail not present in u_Y. However, at nuclear matter density, 0.17 neutron/F^3 the energy of u_{RPA} is 10 MeV higher than that of u_Y out of a total energy of 89 MeV. Comparison of the pseudopotentials shows that u_{RPA} is much larger than the optimal u_Y.

The plasmons, apparently, are more influential in determining the form of the pseudopotential than are the phonons for the low-density neutron system. That is, the $1/r$ term [see Eq. (6)] dominates higher-order terms in the region $r>1$ for a Coulomb system while the $1/r^2$ term only dominates further out for the low-density Yukawa system.

VIII. VIRIAL THEOREM

The virial theorem for any Coulombic system takes a very simple form. The pressure is given by

$$P=-\frac{r_s}{d}\frac{dE}{dr_s}=\frac{2T+V}{d}\quad, \tag{21}$$

where T and V are the kinetic and potential energies. T and V can be computed from the total energy by[34]

$$T=\frac{d(r_sE)}{dr_s}\,,\quad V=\frac{d(r_s^2E)}{r_sdr_s}\,. \tag{22}$$

These equations will be true for variational energies if all parameters in the trial function having units of length have their optimal values. Our results with u_{RPA} will not satisfy these equations as long as r_s appearing in the definition [Eq. (8)] is fixed. The variation of r_s can be done after the fact as follows; suppose we fit the energy to a function[35] $e(r_s)$ and the kinetic energy to $t(r_s)$. Then the variational energy for the density r_s^* using $u_{RPA}(r_s)$ at the density r_s is given by scaling[10] to be

$$E(r_s^*)=s[e(r_s)-t(r_s)]+s^2t(r_s)\,,$$

where $s=r_s/r_s^*$ and the value of r_s which minimizes the energy at r_s^* satisfies the equation

$$r_s^*=-\frac{(d/dr_s)[r_s^2t(r_s)]}{(d/dr_s)\{r_s[e(r_s)-t(r_s)]\}}\,. \tag{23}$$

Now the scaled kinetic and potential energies [e.g., $t(r_s(r_s^*))\times(r_s/r_s^*)^2$] will now satisfy the virial relation no matter what functions $t(r_s)$ and $e(r_s)$ were used. The values of $r_s^*(r_s)$ are given in Table I. Note that the ratio r_s^*/r_s is generally close to unity. In both two and three dimensions $u_{RPA}(r_s)$ is slightly too large[36] at large r_s and too small at small r_s (although some of the variation at the extreme densities is due to an inadequate fit). It appears that $u_{RPA}(r_s)$ is just right for moderate densities and this supports our view u_{RPA} is close to being the optimal pseudopotential. The energy is deepened very little by this scaling procedure, usually less than one standard deviation.

IX. SIZE DEPENDENCE

The dependence of the energy on the size of the system is the largest error in our Monte Carlo calculation. However, this dependence can be calculated in both the high- and low-density limits, and assuming that the error smoothly interpolates between those limits, we can thereby eliminate the major part of it.

Consider a perfectly harmonic crystal with $m^d=N$ particles arranged about N simple cubic (square) lattice sites. For large enough r_s the symmetry of the particles and the pseudopotential can be neglected and the difference between the finite and infinite system potential energy is found to be given very accurately by the expression

$$V_N-V_\infty=\Delta V_N=-w/r_sCN^{3/d}\,, \tag{24}$$

$$w=\begin{cases}0.406\,, & d=2\\ 0.75\,, & d=3\,,\end{cases}$$

where C is the variational parameter of the Gaussian [Eq. (10)]. This difference comes from the interaction of a particle with its own images. The radial distribution function $g(r)$ periodically extended, contains terms $\delta(\vec{r}-\vec{n}L)$, where $\vec{n}$ is an integer vector and depressions around the positions of these δ functions due to the image of the correlation hole about the particle at the origin. But the infinite system $g(r)$ has neither these δ functions nor depressions. The potential energy of the finite system is lower since its structure is closer to the perfect crystal.

This reasoning tells us how to correct the energy in the strong-coupling limit. Using the virial theorem it is easy to show that for large r_s, C will be proportional to $r_s^{1/2}$. Also by the virial theorem the size dependence of the kinetic and potential energies should be equal. Hence

$$E_N-E=-b/r_s^{3/2}N^{3/d}\,, \tag{25}$$

where b is a constant, independent of r_s and N. Note that the above argument should still hold for a strongly correlated fluid.

Now consider the opposite case, a completely degenerate plasma. The size dependence in the Hartree-Fock approximation is given by

$$E_N-E_\infty=\Delta v_N/r_s+\Delta t_N/r_s^2\,. \tag{26}$$

TABLE IV. Energy and size dependence parameters for the fluid phase. b is the size-dependent parameter in Eq. (27). h_0 and h_1 are the kinetic and potential energies in the Hartree-Fock approximation. Δt_N and Δv_N give the size dependence in the Hartree-Fock kinetic and potential energies for the values of N shown [Eq. (26)]. β_1, β_2, and α_4 are the results of the least-squares fit to all the Monte Carlo energies. The other α_i's are to be found by using Eq. (31). f_0^* and f_1^* are the first two terms of the low-density expansion of the Padé approximant with these α_i's and β_i's.

Dimension polarization	2 U	2 P	3 U	3 P
b	2.0	2.0	3.0	3.0
h_0	1.0	2.0	2.2099	3.5080
h_1	−1.2004	−1.6972	−0.91633	−1.1545
N	58	57	162	81
Δt_N	0.01607	0.01124	−0.0513	−0.0576
Δv_N	−0.00501	−0.00762	−0.0363	−0.0647
β_1	1.0026	0.4215	1.15813	0.9321
β_2	0.6167	0.1424	0.34455	0.2020
$\alpha_4 h_0$	−1.3511	−0.1560	−0.2760	−0.1019
f_0^*	−2.1909	2.19	−1.7702	−1.77
f_1^*	1.6102	1.4616	2.870	2.839

Δt_N is an oscillating function of N with an envelope which decays like $1/N$, Δv_N is always negative and decays smoothly like $N^{-2/d}$, again because of the interaction of a particle with its own images. The necessary values of Δt_N and Δv_n are shown in Table IV.

To interpolate between the high- and low-density limit we have used the simplest Padé function in $r_s^{1/2}$, requiring the term in $r_s^{-3/2}$ to vanish at small r_s. Then the size dependence is assumed to be of the form

$$E_N - E_\infty = \Delta t_N/r_s^2 + (r_s/\Delta v_N - N^{3/d} r_s^{3/2}/b)^{-1}, \qquad (27)$$

where b is determined by a nonlinear least-squares fit using the results of several calculations at different values of N and r_s but within the same phase. The value of the fitted b is in Table IV. The corrections in two dimensions are quite small for $N = 58$, about one standard deviation. But in three dimensions they are quite large, ranging from 70 standard deviations at $r_s = 1$ to 5 standard deviations at $r_s = 10$ (with $N = 162$). We believe that the error in the procedure is much smaller than the correction, at least by a factor of 10, because of our success in fitting the results of calculations at smaller N.

In the crystal phase no interpolation is necessary and Eq. (25) was used to determine the size correction, with b determined from several runs at different values of N.

X. EQUATION OF STATE

With the procedures of scaling and correcting for the size dependence described above, we now wish to fit the resulting energies to an analytic expression in order to smooth out fluctuations in the energies and allow the interpolation between and extrapolation beyond the Monte Carlo densities. Padé approximates are a logical choice for an analytic expression since a great deal is known about the form of the energy at high and low densities. At high density the Brueckner[37] expansion about the ideal gas yields asymptotically:

$$E_0 = h_0/r_s^2 + h_1/r_s + O(\ln r_s), \quad r_s \ll 1. \qquad (28)$$

The coefficients h_0, h_1 for the polarized and unpolarized fluid in two and three dimensions are tabulated in Table IV. At low density in the Wigner crystal phase one expects the energy to have the form[28,29]

$$E_0 = \frac{f_0}{r_s} + \frac{f_1}{r_s^{3/2}} + \frac{f_2}{r_s^2} + O(r_s^{-5/2}) + \cdots, \quad r_s \gg 1. \qquad (29)$$

For the crystal the coefficients f_0, f_1, f_2 are given by the anharmonic crystal expansion. See Table V.

TABLE V. Energy expansion in the crystal phase. f_0, f_1, and f_2 are the coefficients in Eq. (29). b is the size-dependence parameter in Eq. (25). The numbers in parentheses represent the standard error in the last digit of our estimate of f_2.

d	b	f_0	f_1	f_2
2	2.5	−2.2122	1.628	0.25(2)
3	3.0	−1.79185	2.65724	−0.73(4)

In order to have the correct limiting form at large r_s we choose our Padé variable to be $x=r_s^{1/2}$. Then a simple form for the fluid energies is

$$E(r_s)=\frac{\sum_{i=0}^{4}\alpha_i x^i}{r_s^2(1+\sum_{i=1}^{2}\beta_i x^i)}. \tag{30}$$

In addition we constrain the α_i's and β_i's to have the Hartree-Fock limiting form [up to but not including the $\ln r_s$ term in Eq. (28)]. This gives four conditions:

$$\begin{aligned}&\alpha_0=h_0\,,\quad \alpha_2=h_1+\beta_2 h_0\,,\\ &\alpha_1=h_0\beta_1\,,\quad \alpha_3=h_1\beta_1\,.\end{aligned} \tag{31}$$

The remaining three parameters (taken to be β_1,β_2,α_4) are determined by a nonlinear least-squares fit[38] to the Monte Carlo fluid energies (after scaling and size corrections). The coefficients are given in Table IV. The chi-square for the fits is very good in two dimensions and reasonable in three dimensions. The density range spanned by our simulations is very large ($1\leq r_s\leq 500$) and the error bars on the energy are quite small, so that the chi-square test is very severe.

Our energy expression must break down at small enough r_s since it does not have a logarithmic term[39]; adding a term proportional to $\ln(r_s)$ did not noticeably improve the fit.

Equation (29) fits the Monte Carlo crystal energies well. In three dimensions our energies agree with the anharmonic crystal calculation of Carr,[28] thus showing that the terms beyond $1/r_s^2$ are small for $r_s>50$. In two dimensions only the harmonic terms have been calculated[29] (f_0 and f_1). f_2 as determined from our variational energies is shown in Table V.

For very low densities the fluid energies were expanded as in Eq. (29). The coefficients called f_i^* (obtained from the α_i's and β_i's) are shown in Table IV. Note that f_0^* is greater than f_0 by roughly 0.021. It is this difference which forces the liquid to crystallize. The second term f_1^* is approximately the same as in the crystal, f_1. Hence the kinetic energy of the liquid and crystal are roughly the same at the same density. But f_1^* is less for the polarized liquid than for the unpolarized liquid which means that the polarized liquid will have a lower energy at large r_s.

XI. ERRORS

We will now try to estimate the errors in the Monte Carlo calculation of the ground-state energy. The total error comes from several different sources and can be broken down as follows:

(a) *Numerical errors*: This category includes round-off error and the error resulting from calculating only an approximation to the "image" potential (see Appendix). Various tests indicate that the cumulative effect of these errors is less than one part in 10^{-5}.

(b) *Convergence error*: This results from not allowing the random walk enough steps to equilibriate and not exploring configuration space fully enough. For the electron plasma this error has not proved to be significant. Occasionally the random walk was allowed to proceed many times further than normal and there was no unexpected change in any of the average quantities.

(c) *Statistical error*: This is tabulated in Tables I–III. The estimate of the statistical error is computed by dividing the entire random walk into roughly 10 equal blocks and finding the variance of the average energy in those blocks. This error can be roughly summarized in the formula

$$\Delta E=0.5[E(r_s)-V_x]/(NM)^{-1/2}\,, \tag{32}$$

where M is the number of moves per particle of the random walk and V_x is the potential energy of the perfect crystal. Since ΔE is proportional to the excess energy, Monte Carlo can be successfully used to estimate very small energy differences. It is interesting to note that if the trial function is improved the coefficient (i.e., 0.5) should become smaller.

(c) *Size dependence*: We have attempted to remove this as discussed above and believe that the remaining size dependence is of the order of ΔE.

(e) *Nonoptimal choice of the pseudopotential*: Our searches in two and three dimensions indicate that this error is quite small and of the order of ΔE. Use of the virial scaling procedure discussed above lowered the energy hardly at all. Extensive searches for a better pseudopotential for Lennard-Jones helium have produced no significant lowering of the energy (less than 0.1 °K). We know from the cusp condition, Eq. (5), that the optimal pseudopotential will depend on spin. Stevens and Pokrant[25] have calculated variational energies with and without a spin-dependent pseudopotential and they find a drop in energy of only 0.0007 at $r_s=5.4$ and a drop of 0.0001 at $r_s=7.9$. Talman[20] gets roughly the same drop.

(f) *Error in choosing the product form for the trial function:* Since the true ground-state energy is unknown this error is difficult to estimate. In the high-density limit Gaskell[19] has shown that u_{RPA} will have a variational energy higher than the ground-state energy by an amount asymptotically equal to

$$E_{\mathrm{RPA}}-E_0=-0.00052\ln(r_s)+0.036+O(r_s\ln(r_s))\,,\qquad r_s\ll 1. \tag{33}$$

In the density regime where the electrons are

strongly coupled but still in the fluid phase, the kinetic energy due to the antisymmetrization is smaller than that due to the pseudopotential. This can be seen by comparing $\bar{k}$ with $\bar{k}_B$ in Table I. Then it is likely that the error in the variational approximation for the fermion plasma is about the same as that in the boson plasma. Exact Green's-function Monte Carlo results for bosons interacting with a Yukawa potential[40] show that in the strongly coupled liquid the variational error is about 5% of the excess energy (ground-state energy minus potential energy of a perfect crystal). In the case of the 3D electron fluid this yields

$$E_{\mathrm{RPA}} - E_0 = 0.05 \times 2.87/r_s^{3/2}, \quad r_s \gg 1. \tag{34}$$

Finally, the exact results for the boson Yukawa crystal[40] show that the error in the variational trial function is smaller than in the liquid, being about 3% of the excess energy. This difference in the accuracy of the trial function in the two phases will cause a major shift in the transition density as discussed below.

In two dimensions the variational approximation may be more accurate since the trial function has the same number of exact properties as in three dimensions, but the configuration space is much reduced. In other words, the number of nearest-neighbor triplets which are left out of the product trial function, compared with the number of pairs is roughly 3 times smaller in two than in three dimensions. Hence the contribution of triplets and higher-order correlations may be much smaller in two dimensions.

To summarize: our variational energies as calculated using Eq. (29)–(31) with the coefficients from Tables IV and V have an error roughly equal to that found in Tables I–III. This estimate encompasses the errors of type (a) through type (e). But the error due to assuming a product trial function as estimated in Eqs. (33) and (34) is much larger. Hence although we have not found the ground-state energy we have obtained a valuable upper bound. The next step in a better calculation of the plasma ground state will clearly involve going beyond the product trial function to include many-body correlations.

XII. COMPARISON WITH OTHER CALCULATIONS

There have been a large number of calculations of the correlation energy of the three-dimensional (3D) electron fluid because of its importance as a model of metals. We will only briefly compare our results with some of these. In Figs. 1 and 2 the solid line is the correlation energy we have found (smoothed and corrected). In general, calculations of the correlation energy can be divided

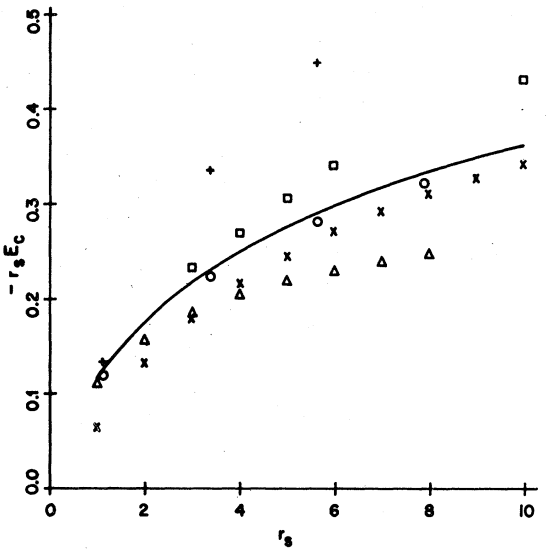

FIG. 1. Minus the correlation energy times r_s vs r_s from our calculation (solid line) compared with other variational calculations. The correlation energy (E_c) is the Hartree-Fock energy minus the ground-state energy in Rydbergs. The solid line is from Eq. (30) and Table IV. The other symbols represent the results of (+) Becker, Broyles, and Dunn (Ref. 23), (□) Monnier (Ref. 24), (△) Talman (Ref. 20), (○) Stevens and Pokrant (Ref. 25), and (×) Lee and Ree (Ref. 42).

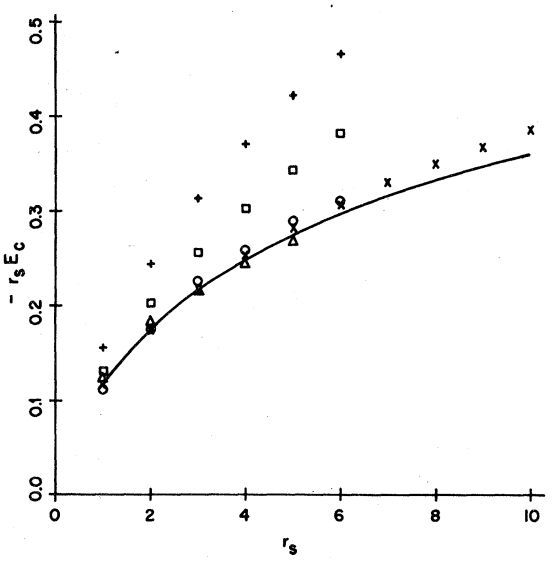

FIG. 2. Minus the correlation energy times r_s vs r_s from our calculation (solid line) compared with perturbational calculations. The symbols represent the results of (+) the RPA approximation Freeman (Ref. 41), (□) Hubbard (Ref. 45), (○) Vashishta and Singwi (Ref. 43), (×) Freeman (e^s) (Ref. 41), and (△) Lowy and Brown (Ref. 44).

into two classes: variational and perturbational. These are shown in Figs. 1 and 2, respectively.

The Monte Carlo calculation of Monnier[24] most resembles the present one. However, in that calculation antisymmetry was only accounted for in an approximate way. It is seen that his results are significantly lower than ours. It is likely that the neglect of the angular portion of the "image" potential and of correlations in $g(r)$ for $r > \frac{1}{2}L$ led to a systematic error. Stevens and Pokrant[25] assumed the trial function was of the product form and then found the energy using the hypernetted chain approximation, the convolution approximation and a "semiclassical" treatment of antisymmetry. The agreement of the energy is quite good, although their energies are significantly higher for $r_s > 5$.

In Fig. 2 are shown the results of various perturbational calculations. The random-phase approximation is seen to be quite poor, giving energies much too low. An improved RPA theory, the coupled-cluster or e^S method[41] gives energies essentially identical to ours for $r_s < 5$, but these energies are definitely too low at $r_s = 10$. A dielectric formulation also gives good agreement for small values of r_s.[44,45]

In the three-dimensional crystal our energies agree within errors to the predictions of the anharmonic crystal series expansion of Carr and are lower than the self-consistent phonon calculation of Glyde *et al.*[46] by roughly $-1.1/r_s^2$.

The accurate agreement at high and low densities with other calculations is a strong vindication of the procedures used to calculate the energy. Four quite different methods now give correlation energies the same to within 0.002 Ry for $r_s < 5$. But we must reemphasize that the Monte Carlo variational method is least accurate in this density range and we believe that it is more reliable and accurate than the other energies shown in Figs. 1 and 2 in the strong-coupling region ($r_s > 5$).

XIII. PHASE TRANSITIONS

Our simulations indicate that at least three phases are stable in the plasma at zero temperature. At low density the crystal phase is of course preferred. We have not investigated the type of spin ordering in the crystal in detail. Preliminary calculations indicate (see Table III) that the energy is insensitive to the spin ordering, in agreement with the anharmonic crystal predictions of Carr. As the density increases, the crystal melts (in both two and three dimensions) and becomes a totally polarized electron fluid. This occurs at a density of $r_s = 67 \pm 5$ in three dimensions (5.4×10^{18} e^-/cm^3) and $r_s = 33 \pm 2$ in two dimensions (1.0×10^{13} e^-/cm^2). Lindemann's quantum rule, which states that the phase transition occurs when the root-mean-square particle displacement from the lattice site equals about 0.30 ± 0.02 of the nearest-neighbor distance, holds for all quantum crystal we have examined.[47]

At a higher density the normal or unpolarized fluid is the stable phase. The polarized-unpolarized transition occurs at a density of $r_s = 26 \pm 5$ in three dimensions (9.2×10^{19} e^-/cm^3) and of $r_s = 13 \pm 2$ in two dimensions (6.7×10^{13} e^-/cm^2). These values of r_s are higher than those calculated by dielectric methods.

The error bars on the above transition densities include all errors except that resulting from the assumption of a product trial function. As mentioned above, it is likely that the product trial function favors the crystal phase. If we boldly extrapolate from the exact results of the boson Yukawa system (where the excess energy is overestimated by 2% in the fluid phase) to the 3D electron system, the polarized fluid-crystal transition shifts to $r_s = 90 \pm 20$ (2.2×10^{18} e/cm^3). Hence it is realistic to say that we have found upper bounds to the crystallization density.

We have not found a physical argument to explain why the polarized liquid is preferred over the normal liquid at low densities in both two and three dimensions. The energy differences between the two phases are always quite small and judging from other phase transitions there must be some rather subtle changes in the local ordering of the liquid. Putting more nodes (via the Slater determinant) into the trial function appears to be a more efficient way of separating the particles at low density than simply increasing the repulsion of the pseudopotential.

The quantum plasma with a uniform background is unstable against collapse at low density. The energy per particle has a minimum at $r_s = 1.5$ in two dimensions and $r_s = 4.2$ in three dimensions. The compressibility is negative at densities below $r_s = 2.1$ in two dimensions and $r_s = 5.4$ in three dimensions, hence lower densities cannot even be metastable. For this reason one cannot meaningfully calculate the widths of the phase transitions. The above remarks only apply if the background's internal energy is independent of density. For all physical systems the internal energy of the background increases rapidly with density and so stabilizes the total system.

These interesting two-dimensional quantum phase transitions occur at too high a density to be observed with electrons on the surface of helium; the helium surface does not remain flat with such a charge density. However, they may be observed among electrons trapped on an inversion layer.

XIV. CONCLUSIONS

Using the powerful fermion Monte Carlo variational method we have been able to calculate very accurate energies for the quantum plasma. The agreement at low density, with the anharmonic crystal expansion and at high density with three other methods is quite reassuring. We have found that an *a priori* pseudopotential (u_{RPA}) gives quite satisfactory energies and considerably reduces the amount of effort needed in the computer simulation. It is probable that analytic three-body correlation functions could be found which would bring the trial functions much closer to the true ground state. One major advantage to the Monte Carlo method is that the search for better trial functions can be carried out without any further approximations. The simulation also generates a great wealth of information about the ground state. We intend to publish a study of some of the data we have obtained from our simulation of the plasma at a future date (these will include the radial distribution function, the structure function and the momentum distribution).

ACKNOWLEDGMENTS

The Commissariat a l'Energie Atomique has supported me with a Joliot-Curie fellowship during the time this research was performed. I wish to thank the Laboratoire de Physique Theorique et Hautes Energies at Orsay for the generous use of their computing facilities and their hospitality and to D. Levesque for his advice and kindness. I have also had fruitful conversations with J.-P. Hansen and G. Patey concerning the research reported here. I am indebted to M. H. Kalos and G. V. Chester for their many suggestions concerning the manuscript. I have also received support from the Department of Energy under Contract No. EY-76-C-02-3077*000.

APPENDIX

The Coulomb potential and the pseudopotential from the random-phase approximation go to zero very slowly for large distances. The problem of how to represent them in a rather small box, by macroscopic standards, with periodic boundary conditions is solved formally by replacing the Coulomb potential between two particles with the "image" potential. Brush *et al.*[31] were the first to use the image potential in the Monte Carlo simulation of the classical one component plasma. In this Appendix we will describe how to handle in a computer simulation the image potential of any potential or pseudopotential which can be expanded in inverse powers of r for large r.

The method is essentially due to Nijboer and deWette.[48] They showed that the "image" potential between two particles having an original interaction of $1/r^n$ can be written

$$\phi(\vec{r}) = \sum_{\vec{\lambda}} f(|\vec{r} - \vec{R}_{\vec{\lambda}}|) + \sum_{\vec{\lambda}} g(k_{\vec{\lambda}}) e^{i\vec{k}_{\vec{\lambda}}\cdot\vec{r}}, \tag{35}$$

where $f(r)$ and $g(k)$ are the functions

$$f(r) = \Gamma(\tfrac{1}{2}n, \alpha r^2)/\Gamma(\tfrac{1}{2}n) r^n,$$

$$g(k) = \begin{cases} \dfrac{\pi^{D/2}(2/k)^{D-n}\Gamma(\frac{1}{2}(D-n), k^2/4\alpha)}{V\Gamma(\frac{1}{2}n)}, & k \neq 0 \\ -\dfrac{2\pi^{D/2}}{(D-n)V\Gamma(\frac{1}{2}n)\alpha^{(D-n)/2}}, & k = 0. \end{cases} \tag{36}$$

$R_{\vec{\lambda}}$ and $k_{\vec{\lambda}}$ are the set of lattice and reciprocal-lattice vectors of the simulation box, V is the volume of the box, $\Gamma(a, z)$ is the imcomplete gamma function. The sum in Eq. (36) is independent of the parameter α which can be varied to change the relative rate of convergence of the series in r and k space. As α goes to zero we recover the original sum of the potential over the images of the other particle and as α goes to infinity the sum in real space vanishes and we observe that the effect of the background is to eliminate the $k_{\vec{\lambda}} = 0$ term from the summation over the Fourier transform of the interaction. The rate of convergence of the two series will be the same for

$$\alpha = \pi/V^{2/d}. \tag{37}$$

Adams and McDonald[49] observed that if α is made large enough all but the first term ($\vec{R}_{\vec{\lambda}} = 0$) in the sum over lattice vectors can be ignored. The sum in k space can then be put into a particularly convenient form for Monte Carlo calculations. In a Monte Carlo simulation we need the potential energy of a single particle. Using Eq. (35) and dropping all terms with $R_{\vec{\lambda}} \neq 0$ this is

$$u_i \equiv \sum_{j\neq i}^{N} \phi(\vec{r}_{ij}) = \sum_{j\neq i}^{N} f(r_{ij}) + \sum_{k\vec{\lambda}} g(k_{\vec{\lambda}})[\rho_{\vec{k}_{\vec{\lambda}}} \exp(-i\vec{k}_{\vec{\lambda}}\cdot\vec{r}_i) - 1] + C_0, \tag{38}$$

where

$$C_0 = \sum_{\vec{k}_{\vec{\lambda}}\neq 0} g_{\vec{k}_{\vec{\lambda}}} - 2\alpha^{n/2}/n\Gamma(\tfrac{1}{2}n) \tag{39}$$

comes from the interaction of particle i with its own images. The $\rho_{\vec{k}}$ are the usual collective coordinates, Eq. (14). The first term in Eq. (38) uses the $N-1$ distances r_{ij} and can be done by tabulating the spherical function $f(r)$. The number of nonzero components of g_k summed in the second

term depends on the accuracy needed in the calculated potential. Let us suppose the vectors in k space are summed out to K_{max}. Then we have found that to minimize the error in the potential one should choose α as

$$\alpha = (K_{max}L/\pi + 1)/3L^2 . \tag{40}$$

Note that this choice is independent of both d and n. The maximum error depends on n, being smaller for smaller values of n, but is independent of d. If we choose $K_{max} = 8\pi/L$ the maximum error in a single term is $10^{-4}/L$ for $n = 1$. This will require 257 points in k space in three dimensions but only 49 in two dimensions.

The random-phase pseudopotential in Eq. (8) or Eq. (18) is not a simple power law. To apply the above formulas, the pseudopotentials were expanded in a Laurent expansion about $k = 0$. In r space this gives an asymptotic expansion, which was found to be accurate for large r ($r > 2$) if only the terms $1/r^p$ were kept where $p < d$. That is, the interaction was assumed to be

$$u(r) = \begin{cases} u_{RPA}(r) , & r < \frac{1}{2}L \\ \sum \beta_i / r^{p_i} , & r > \frac{1}{2}L . \end{cases} \tag{41}$$

Then $f(r)$ and g_k in Eq. (38) were computed as

$$f(r) = \begin{cases} u_{RPA}(r) + \sum_i \beta_i [f(n_i, r) - 1/r^{n_i}] , & r < \frac{1}{2}L \\ 0 , & r > \frac{1}{2}L \end{cases}$$

$$g_k = \sum_i \beta_i g_k(n_i) , \tag{42}$$

where $f(n,r)$ and $g_k(n)$ are defined in Eq. (36). This method works quite well for any interaction that is well represented by an asymptotic expansion outside the simulation box.

---

*Present address: Courant Institute of Mathematical Sciences 251 Mercer St., New York, N. Y. 10011

[1]E. E. Salpeter, Aust. J. Phys. 7, 373 (1954).
[2]M. Cole, Rev. Mod. Phys. 46, 451 (1974).
[3]A. V. Chaplick, Sov. Phys.-JETP 35, 395 (1971); "Proceedings of the International Conference on Electronic Properties of Quasi-Two-Dimensional Systems," Surf. Sci. 58 (1976).
[4]E. P. Wigner, Phys. Rev. 46, 1002 (1934); Trans. Faraday Soc. 34, 678 (1938).
[5]C. M. Care and N. H. March, Adv. Phys. 24, 101 (1975).
[6]F. Bloch, Z. Phys. 57, 549 (1929).
[7]Setsuo Misawa, Phys. Rev. 140, A1645 (1965).
[8]S. F. Edwards and A. J. Hillel, J. Phys. C 1, 61 (1968).
[9]A. W. Overhauser, Phys. Rev. Lett. 3, 414 (1959); Phys. Rev. Lett. 4, 462 (1960); Phys. Rev. 128, 1437 (1962).
[10]W. L. McMillan, Phys. Rev. 138, A442 (1965).
[11]D. M. Ceperley, G. V. Chester, and M. H. Kalos, Phys. Rev. B 16, 3801 (1977).
[12]D. Ceperley and M. H. Kalos, in *Monte Carlo Methods in Statistical Physics*, edited by K. Binder (Springer-Verlag, Berlin, to be published).
[13]N. Metropolis, A. Rosenbluth, M. Rosenbluth, A. H. Teller, and E. Teller, J. Chem. Phys. 21, 1087 (1953).
[14]A. Bijl, Physica 7, 869 (1940); R. B. Dingle, Philos. Mag. 40, 573 (1949); R. Jastrow, Phys. Rev. 98, 1479 (1955).
[15]C. de Michelis and L. Reatto, Phys. Lett. A 50, 275 (1974).
[16]The Euler-Lagrange equation for $u^*(r)$ can be stated as follows: the variational energy of the system with two particles held a fixed distance r apart must equal the unconstrained variational energy. For small r this gives the cusp condition.
[17]D. Bohm and D. Pines, Phys. Rev. 92, 609 (1953).
[18]M. A. Pokrant and F. A. Stevens, Phys. Rev. A 7, 1630 (1973).
[19]T. Gaskell, Proc. Phys. Soc. 77, 1182 (1961); 80, 1091 (1962).
[20]J. D. Tallman, Phys. Rev. A 13, 1200 (1976).
[21]E. Krotscheck, Phys. Rev. A 15, 397 (1977).
[22]D. M. Ceperley, G. V. Chester, and M. H. Kalos, Phys. Rev. D 13, 3208 (1976).
[23]M. S. Becker, A. A. Broyles, and T. Dunn, Phys. Rev. 175, 224 (1968).
[24]R. Monnier, Phys. Rev. A 6, 393 (1972).
[25]F. A. Stevens and M. A. Pokrant, Phys. Rev. A 8, 990 (1973).
[26]J. P. Hansen and D. Levesque, Phys. Rev. 165, 293 (1968).
[27]For the Boltzmann crystal the Euler-Lagrange equation for $\phi(r)$ is the variational energy of the whole system if one particle is held a distance r from its lattice site must equal the unconstrained variational energy. This implies that for large r that $\phi(r) = \exp(-\delta r/r)$ times a function periodic in the lattice where δ is the energy of removing a particle to infinity.
[28]W. J. Carr, Phys. Rev. 122, 1437 (1961).
[29]L. Bonsall and A. A. Maradudin, Phys. Rev. B 15, 1959 (1977).
[30]N. D. Mermin, Phys. Rev. 176, 250 (1968). Note that an infinite two-dimensional lattice is only unstable if $T > 0$.
[31]S. G. Brush, H. L. Sahlin, and E. Teller, J. Chem. Phys. 45, 2102 (1966).
[32]J.-P. Hansen and R. Mazighi, Phys. Rev. A (to be published).
[33]In fact, the image potential of u_{RPA} as described in the Appendix is almost identical to the optimal u_Y.
[34]N. H. March, Phys. Rev. 110, 604 (1958).
[35]The fitting function used for $e(r_s)$ is given by Eq. (30) with the constraints in Eqs. (31). The function for $t(r_s)$ is the derivative of Eq. (30) [as in Eq. (22)].
[36]One can show for very large r_s in three dimensions that $r_s^* = 0.36 r_s$.
[37]M. Gell-Mann and K. A. Brueckner, Phys. Rev. 106, 364 (1957); W. A. Carr and A. Maradudin, Phys. Rev. 133, A371 (1964); D. Y. Kojima and A. Ishihara, Z.

Phys. B 21, 33 (1975); A. Ishihara and T. Toyado, Z. Phys. B 26, 216 (1977); A. K. Rajagopal and J. C. Kimball, Phys. Rev. B 15, 2819 (1977).

[38]For the polarized fluid in two and three dimensions we also demanded that the ratio α_4/β_2 have the same value as in the unpolarized fluid since there were fewer Monte Carlo densities.

[39]A. Ishihara and E. W. Montroll, Proc. Natl. Acad. Sci. 68, 3111 (1971).

[40]D. Ceperley, G. V. Chester, and M. H. Kalos, Phys. Rev. B 17, 1070 (1978).

[41]D. L. Freeman, Phys. Rev. B 15, 5513 (1977).

[42]D. K. Lee and F. H. Ree, Phys. Rev. A 6, 1218 (1972).

[43]P. Vashishta and K. S. Singwi, Phys. Rev. B 6, 875 (1972).

[44]D. N. Lowy and G. E. Brown, Phys. Rev. B 12, 2138 (1975).

[45]K. S. Singwi, M. P. Tosi, R. H. Land, and A. Sjolander, Phys. Rev. 176, 589 (1968).

[46]H. R. Glyde, G. H. Keech, R. Mazighi, and J.-P. Hansen, Phys. Lett. A 58, 226 (1976).

[47]The quantum crystals examined to date are the two isotopes of helium and bosons and fermions interacting with a Yukawa potential. In all of these the crystal melts when Lindemann's ratio equals 0.30 ± 0.02.

[48]B. R. A. Nijboer and F. W. de Wette, Physica 23, 309 (1957).

[49]D. J. Adams and I. R. McDonald, J. Phys. C 7, 2761 (1974).